Progress of Theoretical Physics, Vol. 121, No. 6, June 2009

Time Correlation Calculation Method Based on Delayed Coordinates

Kai Morino,[1] Miki U. Kobayashi[2] and Syuji Miyazaki[1]

[1]*Department of Applied Analysis and Complex Dynamical Systems, Graduate School of Informatics, Kyoto University, Kyoto 606-8501, Japan*
[2]*Research Institute for Mathematical Sciences, Kyoto University, Kyoto 606-8502, Japan*

(Received December 25, 2008)

An approximate calculation method of time correlations by use of delayed coordinate is proposed. For a solvable piecewise linear hyperbolic chaotic map, this approximation is compared with the exact calculation, and an exponential convergence for the maximum time delay M is found. By use of this exponential convergence, the exact result for $M \to \infty$ is extrapolated from this approximation for the first few values of M. This extrapolation is shown to be much better than direct numerical simulations based on the definition of the time correlation function. As an application, the irregular dependence of diffusion coefficients similar to Takagi or Weierstrass functions is obtained from this approximation, which is indistinguishable from the exact result only at $M = 2$. The method is also applied to the dissipative Lozi and Hénon maps and the conservative standard map in order to show wide applicability.

Subject Index: 033

§1. Introduction

One of the most important characterizations of chaotic or stochastic systems is a description of collapses of temporal correlations. Two conventional methods are well known to obtain time correlations analytically. One is based on unstable periodic orbits,[1),2)] the other on Markov partitions.[3),4)] Both are very cumbersome to find. We would like to propose a new method without using unstable periodic orbits or Markov partitions in this paper.

We confine ourselves to discrete chaotic dynamical systems hereafter. Let us consider a chaotic map $x_{n+1} = F(x_n)$ with discrete time $n = 0, 1, 2, \cdots$. For an observable $u_n = h\{x_n\}$, where $h\{x\}$ is a unique function of x, the equation of motion of u is given by $u_{n+1} = \mathcal{L}u_n$ with the time evolution operator $\mathcal{L}$ defined by $\mathcal{L}G(x) = G(F(x))$ for an arbitrary function G of x. By use of the projection operator method proposed by Mori,[5)] the equation of motion is transformed into

$$u_{n+1} = \zeta u_n + \sum_{s=0}^{n-1} \psi_{n-1-s} u_s + f_n, \tag{1·1}$$

with both $\zeta \equiv \langle(\mathcal{L}u_0)u_0\rangle/\langle(u_0)^2\rangle$ and the memory kernel $\psi_n \equiv \langle(\mathcal{L}f_n)u_0\rangle/\langle(u_0)^2\rangle$ defined, and the fluctuating force $f_n = (\mathcal{Q}\mathcal{L})^n\mathcal{Q}\mathcal{L}u_0$ orthogonal to u_0, i.e., $\langle f_n u_0\rangle = 0$, where the projection operator $\mathcal{P}$ is defined as $\mathcal{P}G(x) \equiv x\langle G(x)x\rangle/\langle x^2\rangle$ with $\mathcal{Q} \equiv 1 - \mathcal{P}$. The bracket $\langle\cdots\rangle$ denotes the long time average. The long time average of

both sides of Eq. (1·1) multiplied by u_0 yields

$$\langle u_{n+1}u_0\rangle = \zeta\langle u_n u_0\rangle + \sum_{s=0}^{n-1}\psi_{n-1-s}\langle u_s u_0\rangle. \tag{1·2}$$

The time correlation function of u is given by $C_n = \langle u_n u_0\rangle$, where the vanishing average $\langle u_n\rangle = 0$ is assumed. Equation (1·2) is expressed by C_n as

$$C_{n+1} = \zeta C_n + \sum_{s=0}^{n-1}\psi_{n-1-s}C_s. \tag{1·3}$$

Thus the projection operator method gives us an equation satisfied by the time correlation function in a closed form. However, the memory term in Eq. (1·3) forces us to use a cumbersome procedure for analytical treatments such as the continued fraction expansion.[6)]

One may compare an equation of motion of a damped oscillator $\ddot{y} + \dot{y} + y = 0$ whose phase space is one-dimensional with the equivalent two-dimensional equation of motion $(\dot{y}, \dot{p}) = (p, y + p)$, where the former non-Markov equation becomes the latter Markov one with an extension from the one-dimensional phase space y to the two-dimensional one (y, p). Fujisaka[7)] amplified this idea and proposed a novel method of calculating time correlation functions, where the memory term is ignored and the phase space is suitably extended as explained below. The observable is extended to the linearly independent state vector

$$\boldsymbol{u}\{x\} \equiv (h_1\{x\}, h_2\{x\}, \cdots, h_{M+1}\{x\})^T, \tag{1·4}$$

where $h_1\{x\}$ is identical to the original observable $h\{x\}$. M is the number of new scalar observables $h_2, h_3, \cdots, h_{M+1}$ with vanishing long time averages. The extended state vector $\boldsymbol{u}$ obeys the equation of motion $\boldsymbol{u}_{n+1} = \boldsymbol{\mathcal{L}}\boldsymbol{u}_n$. If M is appropriately chosen, the contribution from the memory term is expected to be negligibly small, so that we have

$$\boldsymbol{u}_{n+1} \approx \hat{\zeta}\boldsymbol{u}_n + \boldsymbol{f}_n \tag{1·5}$$

with

$$\hat{\zeta} \equiv \langle(\boldsymbol{\mathcal{L}}\boldsymbol{u}_0)\boldsymbol{u}_0^T\rangle/\langle\boldsymbol{u}_0\boldsymbol{u}_0^T\rangle. \tag{1·6}$$

The fluctuating force $\boldsymbol{f}_n$ is orthogonal to $\boldsymbol{u}_0$, i.e., $\langle\boldsymbol{f}_n\boldsymbol{u}_0^T\rangle = \boldsymbol{0}$. Equation (1·5) can be written using the time correlation matrix $\hat{C}_n \equiv \langle\boldsymbol{u}_n\boldsymbol{u}_0^T\rangle$ as $\hat{C}_{n+1} \approx \hat{\zeta}\hat{C}_n$, which yields

$$\hat{C}_n \approx \hat{\zeta}^n\hat{C}_0. \tag{1·7}$$

By noting that $\hat{\zeta} = \hat{C}_1\hat{C}_0^{-1}$, the approximate original time correlation function $C_n^{(M)}$ is thus given by 1-1 component of $\hat{C}_n$.

However, the questions on how the phase space is extended and how M is appropriately chosen are still unanswered. In this paper, we confine ourselves to the

time-delayed coordinate as an extended phase space, i.e., $\boldsymbol{u}\{x\} = (h_1\{x\}, h_2\{x\}, \cdots, h_{M+1}\{x\})^T = (x_0, x_1, \cdots, x_M)^T$ with a chaotic map $x_{n+1} = F(x_n)$. Then we control the time delay M, and discuss the ways of convergence of our method to the exact time correlation functions for completely or partially solvable chaotic maps.

This paper is organized as follows. Introducing a solvable model whose time correlation functions are analytically obtained, we compare the exact ones C_n with our approximations $C_n^{(M)}$ and numerically study the M dependence of the differences $|C_n^{(M)} - C_n|$ in §2. And we assume the M dependence of $|C_n^{(M)} - C_n|$ and extrapolate C_n from $C_n^{(M)}$ for small values of n and M, the results of which are compared with numerical evaluations of C_n according to its definition also in §2. As an application of our method, we obtain a complex parameter dependence of diffusion coefficients called *fractal diffusion coefficient* found by Klages and Dorfman[8] without using Markov partitions in §3. In §4, we present the results for the nonhyperbolic Hénon map and the conservative standard map in order to show wide applicability of our method. The final section is devoted to concluding remarks.

§2. Exponential convergence to the exact time correlation functions for a solvable chaotic map

We consider the following piecewise-linear chaotic map:

$$x_{n+1} = f(x_n) = \begin{cases} x_n + 1/2, & (x_n \in [0, 1/2)) \\ 2x_n - 1, & (x_n \in [1/2, 1]) \end{cases} \tag{2·1}$$

whose two-time correlation function $C_n = \langle x_n x_0 \rangle - \langle x_n \rangle^2$ obeys the following recurrence equation:

$$C_{n+2} = \frac{1}{4}\Big(C_{n+1} + C_n\Big) + \frac{1}{144}\Big(-\frac{1}{2}\Big)^n. \tag{2·2}$$

The exact solution is given by

$$\begin{aligned} C_n = {} & \frac{1}{18}\Big(-\frac{1}{2}\Big)^n \\ & + \frac{1}{36\sqrt{17}}\left\{\Big(\frac{1+\sqrt{17}}{8}\Big)^n \frac{37+3\sqrt{17}}{8} - \Big(\frac{1-\sqrt{17}}{8}\Big)^n \frac{37-3\sqrt{17}}{8}\right\}, \end{aligned} \tag{2·3}$$

the values of which are listed in Table I for $n = 0, 1, \cdots, 7$. It can be shown that the values of C_n are rational for an integer n, and there exist three decay rates $(\sqrt{17}-1)/8 \approx 0.390$, $1/2 = 0.5$, and $(\sqrt{17}+1)/8 \approx 0.640$. The last and slowest decay rate $(\sqrt{17}+1)/8 \approx 0.640$ essentially determines the collapse of the time correlation.

Table I. Numerical values of the time correlation function.

n	0	1	2	3	4	5	6	7
C_n	$\frac{11}{144}$	$\frac{1}{144}$	$\frac{1}{36}$	$\frac{1}{192}$	$\frac{23}{2304}$	$\frac{3}{1024}$	$\frac{15}{4096}$	$\frac{211}{147456}$

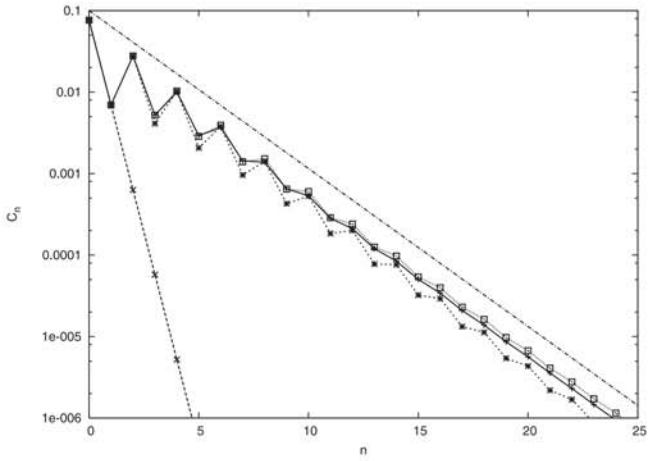

Fig. 1. Analytic solution C_n Eq. (2·3) (+ with solid line) and our approximation $C_n^{(M)}$ for $M = 0$ ($\times$ with dashed line), 1 ($*$ with dashed line) and 2 ($\square$ with dotted line) in Eq. (2·4) are shown in the semilogarithmic plot. The straight dashed-dotted line corresponds to the slowest decay rate $(\sqrt{17}+1)/8 \approx 0.640$ in Eq. (2·3).

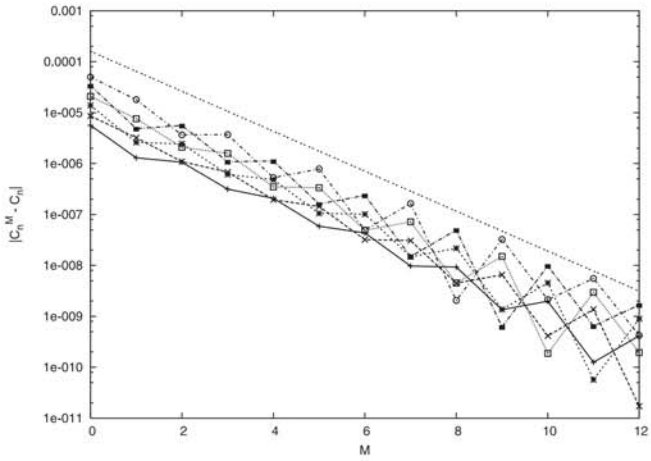

Fig. 2. $|C_n^{(M)} - C_n|$ are plotted against M for $n = 15$ ($\circ$), 16 ($\blacksquare$), 17 ($\square$), 18 ($*$), 19 ($\times$), and 20 ($+$) with a logarithmic vertical axis. The least square method applied to the whole data yields an exponential convergence $|C_n^{(M)} - C_n| \propto \exp(-\alpha M)$ with $\alpha \simeq 0.903$ (straight dotted line).

The correlation matrix $\hat{C}_n$ is determined by $\hat{\zeta}$ and $\hat{C}_0$ as

$$\hat{C}_n = \hat{\zeta}^n \hat{C}_0, \tag{2·4}$$

where the 1-1 element of $\hat{C}_n$ is the approximate time correlation function $C_n^{(M)}$. We compare the analytic solution Eq. (2·3) with our approximation for $M = 0, 1, 2$ in Eq. (2·4) in Fig. 1. For a fixed M, $C_n^{(M)}$ is equal to C_n for $n = 0, 1, \cdots M+1$, and for a fixed n, $C_n^{(M)}$ approaches to C_n, as M is increased. The M dependence of the difference $|C_n^{(M)} - C_n|$ is depicted for $n = 15, 16, 17, 18, 19$, and 20 in Fig. 2. For a fixed n, $C_n^{(M)}$ oscillates with period two as a function of M, so that we decompose Fig. 2 into Fig. 3 for even M and Fig. 4 for odd M. We see that the even-even and the odd-odd combinations for n and M yield the better exponential convergence

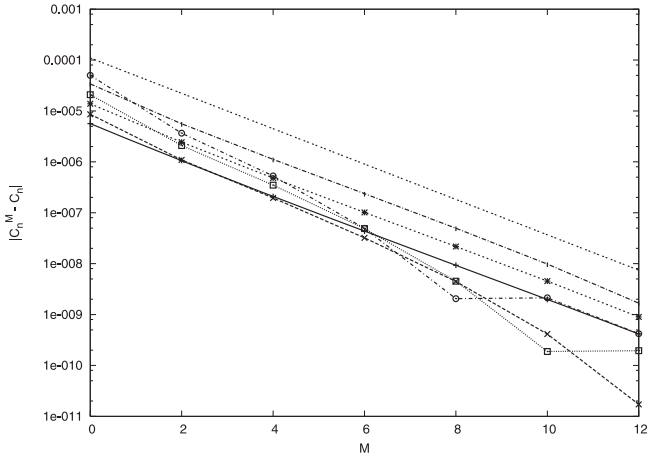

Fig. 3. $|C_n^{(M)} - C_n|$ are plotted against even M for $n = 15$ ($\circ$), 16 ($\blacksquare$), 17 ($\square$), 18 ($*$), 19 ($\times$), and 20 ($+$) with a logarithmic vertical axis. The least square method applied to the data for even n yields the better exponential convergence $|C_n^{(M)} - C_n| \propto \exp(-\alpha M)$ with $\alpha \simeq 0.800$ (straight dotted line).

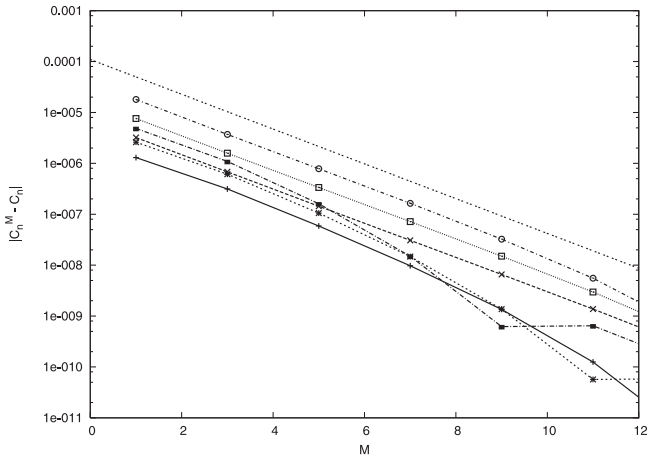

Fig. 4. $|C_n^{(M)} - C_n|$ are plotted against odd M for $n = 15$ ($\circ$), 16 ($\blacksquare$), 17 ($\square$), 18 ($*$), 19 ($\times$), and 20 ($+$) with a logarithmic vertical axis. The least square method applied to the data for odd n yields the better exponential convergence $|C_n^{(M)} - C_n| \propto \exp(-\alpha M)$ with $\alpha \simeq 0.787$ (straight dotted line).

$|C_n^{(M)} - C_n| \propto \exp(-\alpha M)$.

Using the exponential convergence, we can approximate the time correlation function by the extrapolation $C_n^{(\infty)}$ as

$$C_n^{(\infty)} = C_n^{(M)} \pm e^{-\alpha M + B}, \tag{2·5}$$

where the sign in front of the exponential function depends on n, and the real parameters α and B are determined from the least square method applied to $C_n^{(M)}$ at several small values of M for a fixed n.

For a fixed odd (even) n, $C_n^{(\infty)}$ is obtained from the extrapolation using the data $C_n^{(M)}$ at $M = 1, 3, 5, 7, 9$ $(2, 4, 6, 8, 10)$, and compared with the exact value in Table

Table II. Comparison between the extrapolation $C_n^{(\infty)}$ derived from Eq. (2·5) and the exact value C_n given by Eq. (2·3).

n	$C_n^{(\infty)}$ (extrapolation)	C_n (exact)
20	5.653e-006	5.647e-006
25	6.020e-007	6.008e-007
30	6.503e-008	6.494e-008
35	7.029e-009	6.986e-009
40	7.545e-010	7.527e-010
45	8.185e-011	8.106e-011
50	8.768e-012	8.730e-012

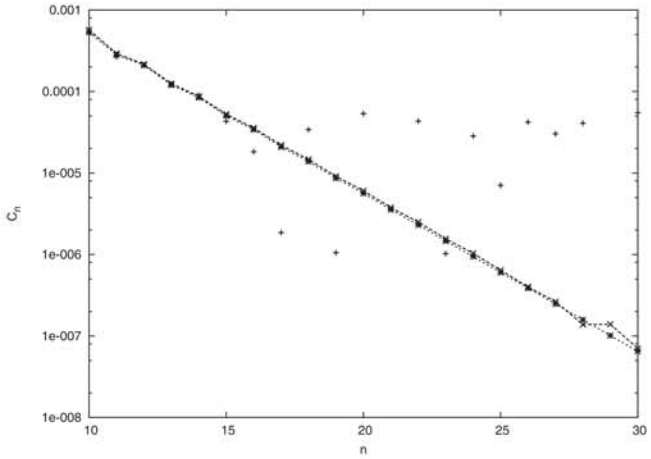

Fig. 5. Comparison between the numerically evaluated time correlation function based on the definition C_n^{num} (+), our approximation $C_n^{(\infty)}$ ($\times$ with a dashed line), and the exact one C_n ($*$ with a dotted line).

II. A good agreement is found, where the convergence rate α depends on n, e.g., $\alpha \simeq 0.784$ for $n = 20$ and $\alpha \simeq 0.772$ for $n = 25$.

We also compare the direct numerical simulation based on the definition of the time correlation function with the exact one C_n and our approximation C_n^{∞} in Fig. 5, where the averages along the 9×10^6 time steps after some initial transient states in the numerical simulation are used to evaluate C_n^{num}, and $C_n^{(\infty)}$ is extrapolated from not the exact but numerically evaluated $C_n^{(M)}$ for $M = 1, 3, 5$ and for $M = 2, 4, 6$ in our approximation. The convergence rates $\alpha \simeq 0.638$ at $n = 7$ and 0.625 at $n = 8$ are used for all odd values and all even values of n.

We see that the direct numerical simulation starts to deviate largely from the exact value at $n = 15$, which is considered to depend on the whole length of the time steps. In contrast, our approximation is in good agreement with the exact value.

§3. An application — Irregular parameter dependence on diffusion coefficients in chaotic diffusion

Diffusion phenomena are characterized by the linear growth of the mean square displacement $\langle (x_t - x_0)^2 \rangle = 2Dt$, where D is called the diffusion coefficient. Diffusion

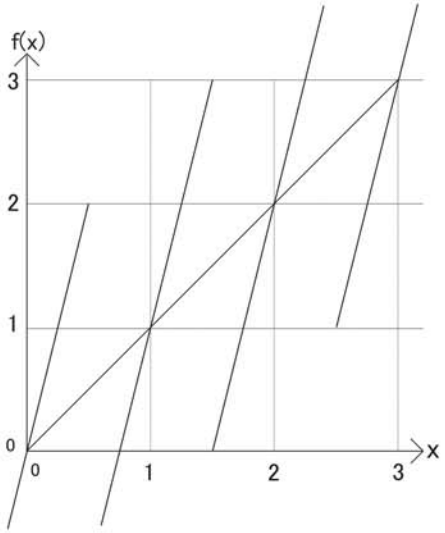

Fig. 6. Map given by Eq. (3·1) at $a = 4$.

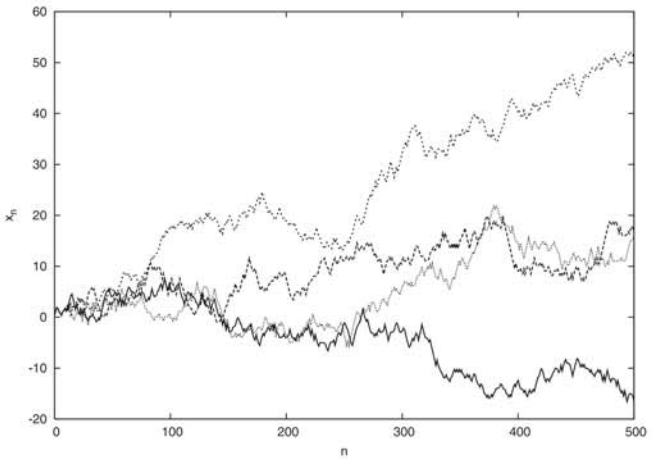

Fig. 7. x_n vs n by iteration of the map given by Eq. (3·1) at $a = 3.2$. Four nearby initial points diffuse over time.

is caused by stochastic noise such as Brownian motions or by chaotic dynamics. Here, we confine ourselves to the latter case, chaotic diffusion also known as deterministic diffusion.

Let us consider the following chaotic one-dimensional map shown in Fig. 6:

$$x_{n+1} = f(x_n) = \begin{cases} a(x_n - N) + N, & x \in A_N, \\ a(x_n - N - 1) + N + 1, & x \in B_N, \end{cases} \tag{3·1}$$

where $N \in \boldsymbol{N}$, $A_N = (N, N + \frac{1}{2}]$, $B_N = (N + \frac{1}{2}, N + 1]$, and a is a real parameter with $a > 2$. As shown in Fig. 7, the nearby initial points diffuse by iteration of the chaotic map without any stochastic factor.

Position x_n is decomposed into an integer part X_n and fractional part x'_n. The new dynamics are given by $N_{n+1} = N_n + \Delta(x'_n)$ and $x'_{n+1} = g(x'_n)$, where $\Delta(x'_n) =$

$\lfloor f(x'_n) \rfloor$ and $g(x'_n) = f(x'_n) - \lfloor f(x'_n) \rfloor$. $\Delta(x'_n)$ can be considered as velocity. In this case, the diffusion coefficient is given by

$$D = \lim_{N\to\infty} \frac{1}{2N} \left\langle \left(\sum_{n=0}^{N-1} x_n - N\langle x \rangle \right)^2 \right\rangle \tag{3·2}$$

$$= \frac{C_0}{2} + \sum_{n=1}^{\infty} C_n \quad , \tag{3·3}$$

where C_n is given by the two-time correlation functions of the velocity $\Delta(x'_n)$. Exact calculations of C_n and D are possible for integer values of a mentioned later and for countable numbers of values of a using Markov partitions. For example, we divide the unit interval $I = [0, 1)$ into four subintervals $I_1 = [0, 1/4)$, $I_2 = [1/4, 1/2)$, $I_3 = [1/2, 3/4)$ and $I_4 = [3/4, 1)$ at $a = 4$ shown in Fig. 6. For the dynamics of the fractional part, $I = I_1 \cup I_2 \cup I_3 \cup I_4 = g(I_i)$ is satisfied for $i = 1, 2, 3$, and 4. Note that $I = I_i \cap I_j = \phi$ for $i \neq j$. The iteration between the subintervals is specified by the transition matrix or the matrix representation of the Frobenius-Perron operator H, whose element is given by $H_{ij} = 1/4$ for all combinations of i and j. We can assign the velocity $u_i = \Delta(I_i)$ as a dynamical valuable with each subinterval I_i for $i = 1, 2, 3$, and 4 with $u_1 = 0$, $u_2 = 1$, $u_3 = -1$, and $u_4 = 0$. Large deviation statistics and time correlation functions of the velocity are obtained from H and its generalization. As described by Yoshida et al.,[9] the Markov partition at $a = 1 + \sqrt{3}$ is given by $I'_1 = [0, 1/(1 + \sqrt{3}))$, $I'_2 = [1/(1 + \sqrt{3}), 1/2)$, $I'_3 = [1/2, 1 - 1/(1 + \sqrt{3}))$, and $I'_4 = [1 - 1/(1 + \sqrt{3}), 1)$ with $g(I'_1) = g(I'_4) = I$, $g(I'_2) = I'_1$, and $g(I'_3) = I'_4$. Note that $I = I'_1 \cup I'_2 \cup I'_3 \cup I'_4$ and $I = I'_i \cap I'_j = \phi$ for $i \neq j$. The elements of the matrix representation of the Frobenius-Perron operator H are given by $H_{k2} = H_{l3} = 0$ for $k = 2, 3, 4$ and $l = 1, 2, 3$, $1/(1 + \sqrt{3})$ otherwise. It is a cumbersome procedure to find the values of a at which the Markov partition is obtained. The situation is similar to the method of finding unstable periodic orbits. Indeed, most of the edges of the subintervals are unstable periodic orbits. The dimension of H, which is equal to the number of partitions, and the elements of H depend very sensitively on the parameter a. Not only H but also the diffusion coefficient D sensitively depends on the parameter a, which was first found by Klages and Dorfman[8] as the *fractal diffusion coefficient*. Similar irregular parameter dependences of diffusion coefficients are observed in several studies.[10),11)]

Our approximation proposed in the present paper does not need Markov partitions, so the irregular parameter dependence of the diffusion coefficient can be obtained much more easily than in the preceding studies.[8),9)] Let the observable of concern u in Eq. (1·1) be the velocity Δ. We approximate C_n by $C_n^{(M)}$ by use of Eq. (1·7) and obtain D from Eq. (3·3). The parameter a dependence of the diffusion coefficient D obtained by our approximation is shown in Fig. 8 for $M = 0, 1$, and 2. Only at $M = 2$ is the result indistinguishable from the exact result.[8] Note that $\hat{C}_n$ is always a $(M + 1) \times (M + 1)$ matrix with constant dimension for all a. Note that direct numerical simulations based on the definition of the diffusion coefficient cannot follow the exact irregular parameter dependence similar to Takagi or Weierstrass

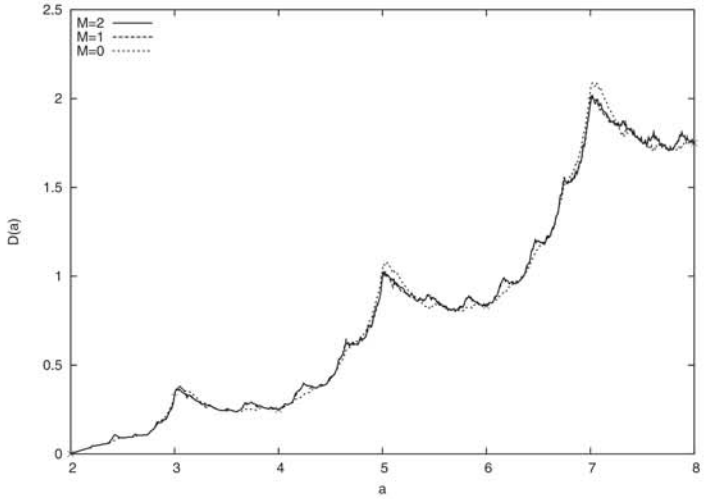

Fig. 8. Irregular parameter dependence of diffusion coefficients obtained by our approximation for $M = 0$ (dotted line), $M = 1$ (dashed line), and $M = 2$ (solid line). The exact result obtained by Klages and Dorfman[8] is indistinguishable from our result for $M = 2$. The exact results for even and odd values of a given by Eqs. (3·4) and (3·5) are also plotted with symbols $\times$ and $+$, respectively.

functions, but a rough dependence.

Analytical results for integer values of a are known,[12)–14)] so we can discuss how our approximation converges to the exact result. For even numbers of a,

$$\begin{cases} C_0 = \frac{(a-1)(a-2)}{12}, \\ C_n = 0, \qquad (n \geq 1) \\ D = \frac{(a-1)(a-2)}{24}, \end{cases} \tag{3·4}$$

and for odd numbers of a,

$$\begin{cases} C_0 = \frac{(a-1)(a^2-2a+3)}{12a}, \\ C_n = \left(\frac{1}{a}\right)^{n+1}\left(\frac{a-1}{2}\right)^3, \quad (n \geq 1) \\ D = \frac{(a^2-1)}{24}, \end{cases} \tag{3·5}$$

hold, which are plotted with symbols $\times$ and $+$, respectively, in Fig. 8. The differences $|C_n^{(M)} - C_n|$ are plotted against M for $n = 5, 6, 7, 8, 9$, and 10 at $a = 11$ in Fig. 9 as a semilogarithmic plot. Exponential convergences $|C_n^{(M)} - C_n| \sim B \exp(-\alpha_a M)$ are observed. For large a, α_a approaches $\alpha_\infty \simeq 0.98$. The differences $\alpha_a - \alpha_\infty$ are plotted against a in Fig. 10 as a logarithmic plot. An algebraic dependence $\alpha_a - \alpha_\infty \propto a^{-\gamma}$ with $\gamma \simeq 2.1$ is observed. The differences $|D_M - D|$ are plotted against M for $a = 5, 7, 9, 11, 73$, and 143 in Fig. 11 as a semilogarithmic plot, where D_M is obtained from our approximation and D is the exact value. Exponential convergences $|D_M - D| \sim B \exp(-\beta_a M)$ are observed. The parameter a dependence of β_a is plotted in Fig. 12. A logarithmic dependence $\beta_a \simeq 0.97 \log a + 0.82$ is observed. Note that $\log a$ is nothing but the Lyapunov exponent of the chaotic map given by Eq. (3·1).

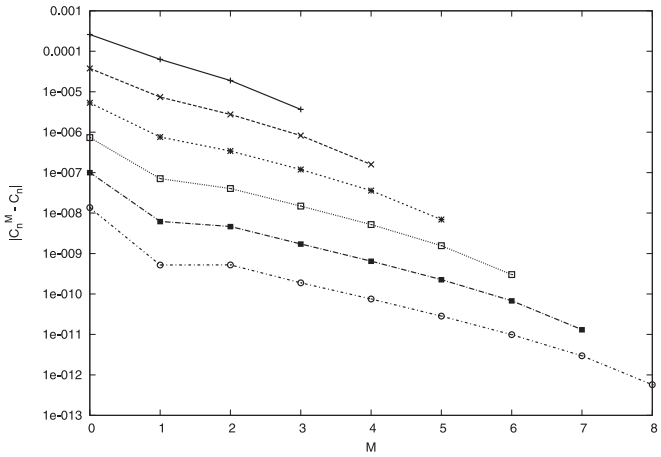

Fig. 9. The differences $|C_n^{(M)} - C_n|$ are plotted against M for $n = 5$ (+), $n = 6$ (×), $n = 7$ (∗), $n = 8$ (□), $n = 9$ (■), and $n = 10$ (○) at $a = 11$ as a semilogarithmic plot.

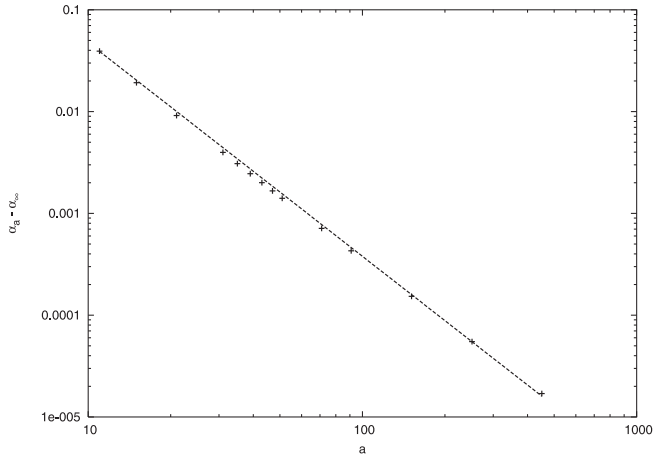

Fig. 10. The differences $\alpha_a - \alpha_\infty$ are plotted against a as a logarithmic plot (+). An algebraic dependence $\alpha_a - \alpha_\infty \propto a^{-\gamma}$ with $\gamma \simeq 2.1$ is drawn with a dotted line.

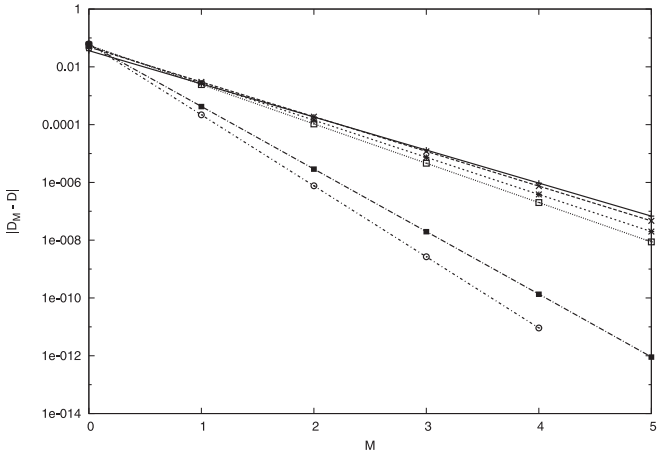

Fig. 11. The differences $|D_M - D|$ are plotted against M for $a = 5$ (+), $a = 7$ (×), $a = 9$ (∗), $a = 11$ (□), $a = 73$ (■), and $a = 143$ (○) as a semilogarithmic plot.

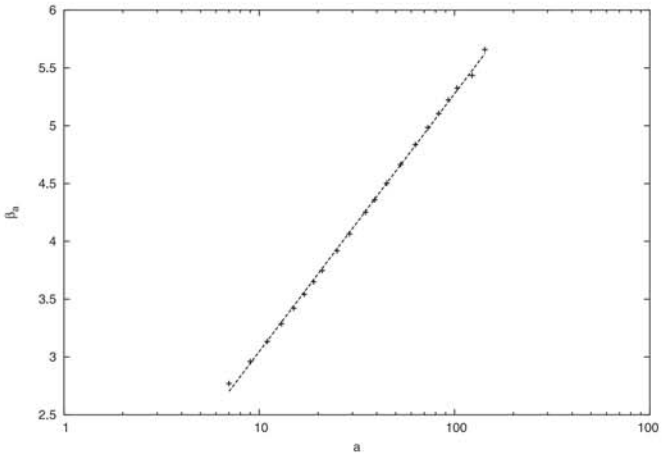

Fig. 12. The parameter a dependence of β_a is plotted as symbols (+). A logarithmic dependence $\beta_a \simeq 0.97 \log a + 0.82$ is drawn with a dotted line.

§4. Other examples

In this section, we present the results for the nonhyperbolic Hénon map and the conservative standard map in order to show wide applicability of our method.

Hata and his collaborators compared the spectrum of singularities, the generalized dimensions and entropies obtained by direct numerical simulations with those obtained by the approximation by use of the unstable periodic points for the Lozi and Hénon maps.[15] Good and poor quantitative agreements were observed, respectively, for the hyperbolic Lozi map and for the nonhyperbolic Hénon map.

The Lozi map[16] is given by $(x_{n+1}, y_{n+1}) = (f(x_n)+by_n, x_n-1/2)$ with $f(x) = \beta x$ for $(0 \leq x < 1/2)$, $\beta(1-x)$ for $(1/2 \leq x < 1)$. We set the parameters as $\beta = (1+\sqrt{5})/2$ and $b = -0.3$. The Hénon map[17] is given by $(x_{n+1}, y_{n+1}) = (1-ax_n^2+y_n, bx_n)$. We set the parameters as $a = 1.4$ and $b = 0.3$. The choice of the parameter, which yields a single-piece chaotic attractor for both maps, is the same as that by Hata and his collaborators.[15] We obtain the two-time correlation function $C_n = \langle x_n x_0 \rangle - \langle x_n \rangle^2$ by direct numerical simulations and our approximation $C_n^{(M)}$. We plot $|C_n^{(M)} - C_n|$ against M for the Hénon map at $n = 10(+), 11(\times), 12(*), 13(\square)$, and $14(\blacksquare)$ and for the Lozi map at $n = 10(\circ), 11(\bullet), 12(\triangle), 13(\blacktriangle)$, and $14(\triangledown)$ in Fig. 13. Even though the agreements between $C_n^{(M)}$ and C_n for the Lozi map are better than those for the Hénon map, $|C_n^{(M)} - C_n|$ becomes smaller as M is increased also for the Hénon map. Note that Markov partitions for the nonhyperbolic Hénon map seem impossible in order to obtain the correlation function.

Next, we take the conservative standard map $(X_{n+1}, P_{n+1}) = (X_n + P_{n+1}, P_n + A\sin(2\pi X_n))$ and consider the diffusion in the momentum direction. The diffusion coefficient of the ensemble of the chaotic orbit is defined by $D = \lim_{T\to\infty}\langle (P_T(i) - P_0(i))^2 \rangle$, where the average $\langle \cdots \rangle$ is taken over the ensemble of i orbits. Applying the Fourier-path integral method, Meiss and his collaborators[18] derived an analytic expression for the diffusion coefficient D as

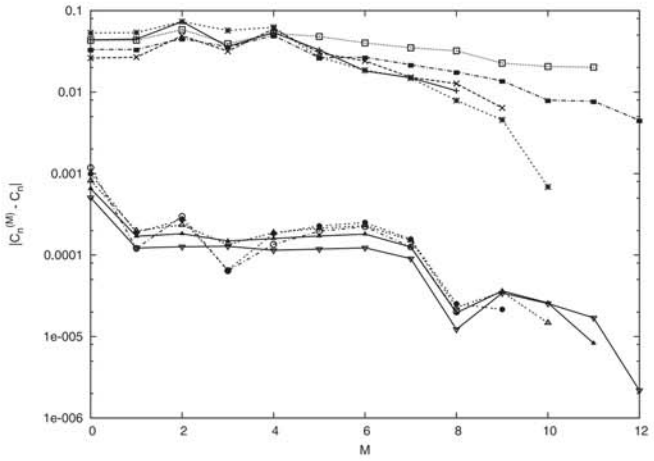

Fig. 13. $|C_n^{(M)} - C_n|$ are plotted against M for the Hénon map at $n = 10(+), 11(\times), 12(*), 13(\square)$, and $14(\blacksquare)$ and for the Lozi map at $n = 10(\circ), 11(\bullet), 12(\triangle), 13(\blacktriangle)$, and $14(\triangledown)$.

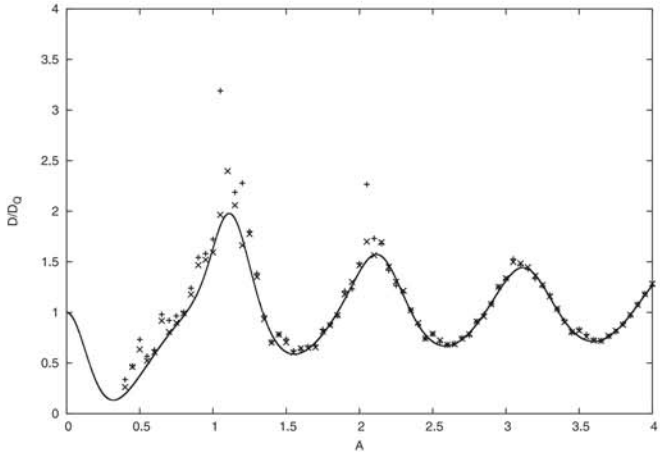

Fig. 14. Normalized diffusion coefficients D/D_Q in the momentum direction are plotted against the parameter A of the standard map for the direct numerical simulation $(+)$ and for our method with $M = 5$ $(\times)$. The theoretical approximation (4·1) is drawn with a solid line.

$$\frac{D}{D_Q} = \frac{1 - 2J_1^2(2\pi A) - J_2^2(2\pi A) + 2J_3^2(2\pi A)}{(1 + J_2(2\pi A))^2}, \tag{4·1}$$

where $J_n(x)$ is the n-th order Bessel function and $D_Q = A^2/4$. We plot the theoretical approximation (4·1) with a solid line and the parameter dependence of D/D_Q obtained from direct numerical simulations with the symbol $(+)$ in Fig. 14. Remarkable deviations are observed around $A = 1$, $A = 2$, and $A = 3$, where the anomalous diffusion caused by accelerator modes occurs.[19)–21)] For the two-time correlation function $C_n = \langle x_n x_0 \rangle - \langle x_n \rangle^2$ with $x_n = P_{n+1} - P_n$, we calculate C_n^M using our approximation. Then we obtain the diffusion coefficient D using Eq. (3·3) for $M = 5$. We plot the parameter dependence of D/D_Q obtained from our approximation as the symbol $(\times)$ in Fig. 14. Good agreements with Eq. (4·1) are observed except for the regions of anomalous diffusion.

Venegeroles analytically calculated the leading Pollicott-Ruelle resonance, whose

wave number dependence determines the diffusion coefficients, for the standard map and other twist maps.[22] His theoretical approximation is very similar to Eq. (4·1). He compared his analytical parameter dependence of the diffusion coefficient derived from the Pollicott-Ruelle resonance with direct numerical simulations. Good agreements similar to our results shown in Fig. 14 were observed.

§5. Concluding remarks

In the present paper, we proposed an approximate calculation method of time correlations by use of a delayed coordinate, which is a special case of the method proposed by the preceding works.[7),23)]

For a solvable piecewise linear hyperbolic chaotic map, we compare our approximation with the exact calculation and find the exponential convergence for the maximum time delay M. Using this exponential convergence, we can extrapolate from our approximation for the first few values of M to the exact result for $M \to \infty$. We also show that this extrapolation is much better than direct numerical simulations based on the definition of the time correlation function. It seems impossible to show how the approximation proposed by the preceding studies[7),23)] converges to the exact result in general cases except for the delayed coordinate.

As an application, we obtain the irregular parameter dependence of diffusion coefficients using our method. Our approximation is indistinguishable from the exact result only at $M = 2$. Furthermore, our method does not need any cumbersome procedure to find a Markov partition. Note that direct numerical simulations based on the definition of the diffusion coefficient cannot follow the exact irregular parameter dependence similar to Takagi or Weierstrass functions, only a rough and rather smooth dependence.

The general theoretical derivation of the convergence rates from our approximation to the exact result is still an open question. The convergence rate α in §2 has no simple relationship with the three decay rates in Eq. (2·3) or with the Lyapunov exponent. Numerical results in §3 imply that $\alpha_a \sim 1 + 1/a^2$ and $\beta_a \sim \lambda + \text{const}$ approximately hold, where $\lambda = \log a$ is the Lyapunov exponent. The reason why these parameter dependences of the convergence rates hold is still unclear.

We also presented the results for the dissipative Lozi and Hénon maps and the conservative standard map in order to show the wide applicability of our method.

We considered here exponential time correlation decays only. Our approximation should be generalized for intermittent signals with an algebraic time correlation decay.

Acknowledgements

This work was supported by a Grant-in-Aid for Scientific Research (c) (No. 20540376) and by the Postdoctoral Fellowship of the Global Centers of Excellence Program "Fostering top leaders in mathematics — broadening the core and exploring new ground" at Kyoto University. We thank Dr. Ryuji Ishizaki for illuminating discussions. We also thank an anonymous referee for introducing the related paper[22]

to us. This paper is dedicated to Dr. Hirokazu Fujisaka who passed away suddenly on August 21, 2007.

References

1) P. Cvitanovic, R. Artuso, P. Dahlqvist, R. Mainieri, G. Tanner, G. Vattay, N. Whelan and A. Wirzba, *Chaos: Classical and Quantum*, `http://www.nbi.dk/ChaosBook/`
2) H. H. Rugh, Nonlinearity **5** (1992), 1237.
3) D. Ruelle, Phys. Rev. Lett. **56** (1986), 405.
4) M. Pollicott, Inventiones mathematicae **81** (1985), 413.
5) H. Mori, Prog. Theor. Phys. **33** (1965), 423.
6) H. Mori, Prog. Theor. Phys. **34** (1965), 399.
7) H. Fujisaka, Prog. Theor. Phys. **114** (2005), 1.
8) R. Klages and J. R. Dorfman, Phys. Rev. Lett. **74** (1995), 387.
9) M. Yoshida, S. Miyazaki and H. Fujisaka, Phys. Rev. E **74** (2006), 026204.
10) K. Tanimoto, T. Kato and K. Nakamura, Phys. Rev. B **66** (2002), 012507.
11) T. Harayama and P. Gaspard, Phys. Rev. E **64** (2001), 036215.
12) S. Grossmann and H. Fujisaka, Phys. Rev. A **26** (1982), 1779.
13) H. Fujisaka and S. Grossmann, Z. Phys. B **48** (1982), 261.
14) R. Klages, *Deterministic diffusion in one-dimensional chaotic dynamical systems* (Wissenschaft and Technik-Verlag, Berlin, 1996).
15) H. Hata, T. Morita, K. Tomita and H. Mori, Prog. Theor. Phys. **78** (1987), 721.
16) R. Lozi, J. de Phys. **39** (1978), 9.
17) M. Hénon, Commun. Math. Phys. **50** (1976), 69.
18) J. D. Meiss, J. R. Cary, C. Grebogi, J. D. Crawford, A. N. Kaufman and H. D. I. Abarbanel, Physica D **6** (1983), 375.
19) Y. H. Ichikawa, T. Kamimura and T. Hatori, Physica D **29** (1987), 247.
20) R. Ishizaki, T. Horita, T. Kobayashi and H. Mori, Prog. Theor. Phys. **85** (1991), 1013.
21) R. Ishizaki, T. Horita and H. Mori, Prog. Theor. Phys. **89** (1993), 947.
22) R. Venegeroles, Phys. Rev. Lett. **99** (2007), 014101.
23) M. U. Kobayashi and H. Fujisaka, Prog. Theor. Phys. **115** (2006), 701.